RSC Advances

PAPER

View Article Online
View Journal | View Issue

Cite this: *RSC Adv.*, 2015, **5**, 51027

Magnetic nano-sized cadmium ferrite as an efficient catalyst for the degradation of Congo red in the presence of microwave irradiation

Wen Shi, Xueyan Liu, Tingting Zhang, Qiong Wang and Lei Zhang*

Received 26th April 2015
Accepted 2nd June 2015

DOI: 10.1039/c5ra07591b

www.rsc.org/advances

A highly active nano-sized $CdFe_2O_4$ catalyst was prepared by a hydrothermal process and characterized by X-ray diffraction (XRD), scanning electronic microscopy (SEM), BET specific surface area method, and vibrating sample magnetometer (VSM) at room temperature. Application of the microwave-induced catalytic degradation method in the abatement of Congo red (CR) using the magnetic catalyst was studied. The degradation ratio of CR with $CdFe_2O_4$ reached 94.4% with 10 min microwave irradiation (MW), proving $CdFe_2O_4$ to be an excellent microwave catalyst. The intermediate products from CR degradation were investigated by UV-Vis, HPLC and ion chromatography. The reaction kinetics, effects of different ion species (SO_4^{2-}, NO_3^-, HCO_3^-, and CH_3COO^-), pH of the solution, dye initial concentration, dosage of catalyst, as well as degradation mechanism were comprehensively studied. Radical trapping studies and the fluorescence technique revealed the holes (h^+) and hydroxyl radicals ($^{\bullet}OH$) were involved as the main active species in the reaction. The band structure of $CdFe_2O_4$ was analyzed by UV-Vis diffuse reflectance spectroscopy and Mott–Schottky measurements. The mechanism of the degradation was discussed in detail. This work can provide an effective technology for dye wastewater treatment.

1. Introduction

Synthetic dyestuffs are used extensively in textile, paper-making, and printing industries and dyehouses. The effluents of these industries are highly colored and the disposal of these wastes into receiving waters can cause damage to the environment. The dyes generally have complex aromatic structures and thus most of them are highly resistant to breakdown by chemical, physical, and biological treatments.[1,2] Microwave techniques have been applied in various fields, such as organic synthesis,[3,4] analysis,[5] and military and environmental engineering.[6,7] Researchers have focused on the application of MW irradiation in environmental wastewater treatment,[8–10] particularly in the degradation of dyes with complex aromatic structures, which are toxic and nondegradable.[11,12] The microwave-assisted degradation technique for pollutants can potentially reduce reaction time.

Over the past decade, MW absorbing materials, known as dielectrics, have been the focus of much attention, particularly for their significant roles in wastewater treatment. Materials, such as activated carbon,[13,14] transition metal oxide,[15,16] CNTs[17,18] and polymers,[19] are commonly used in microwave-assisted degradation of organic pollutants. Among MW absorbents, ferrites are the most promising.[20] Ferrite, which derived from iron oxides, has attracted great interest for its strong absorption ability of microwave. Some ferrites as $MeFe_2O_4$ (Me = Zn, Mn, Co, Ni, Cu, Mg, *etc.*), appeared to be especially efficient for the degradation and removal of organic pollutants.[21–26] However, the performance of nanoscale ferrites in MW-induced degradation process is still needed further research.

Now, we were interested in exploring another member of ferrites, magnetic $CdFe_2O_4$. $CdFe_2O_4$ has normal spinel structure, excellent gas-sensing properties,[27] better charge transport characteristics and small bandgap (1.97 eV).[28] Within literature, most of the studies discussed its applications as gas-sensing materials, but much less attention is given for dye degradation systems. To the best of our knowledge, there is no report on the systematic investigation on dye degradation using nano-sized magnetic $CdFe_2O_4$ as MW absorbing material.

In the present work, $CdFe_2O_4$ was prepared by a one-step hydrothermal method. The catalytic activities of $CdFe_2O_4$ were investigated by degradation of CR solution under MW. The focus was concentrated on below aspects: (1) exploring potential possibility about MW-induced $CdFe_2O_4$ catalytic degradation of dye; (2) identifying intermediates *via* HPLC and ionic chromatogram techniques and proposing MW-induced degradation mechanism based on the exploration of generating chemically-active species.

2. Experimental section

2.1. Chemicals

The target dye CR was purchased from Sinopharm Chemical Reagent Co. Ltd., and used without further purification. All

College of Chemistry, Liaoning University, 66 Chongshan Middle Road, Shenyang 110036, People's Republic of China. E-mail: zhanglei63@126.com; Fax: +86 24 62202380; Tel: +86 24 62207809

chemicals used in this experiment were analytical grade. Deionized water was used throughout the experiments.

2.2. Synthesis and characterization of $CdFe_2O_4$

$CdFe_2O_4$ nanoparticles were synthesized using a hydrothermal process. $Cd(NO_3)_2 \cdot 4H_2O$ (1.2339 g, 0.004 mol) and $Fe(NO_3)_3 \cdot 9H_2O$ (3.2320 g, 0.008 mol) were dissolved in 80 mL of ethanol under continuous stirring to get a homogeneous suspension. The solution was then transferred into a 100 mL Teflon lined stainless-steel autoclave, which was sealed and maintained at 180 °C for 10 h. After allowing the reactor to cool down to room temperature, the precipitate was separated from solution by centrifugation, washed with deionized water and dried at 60 °C for 12 h.

The morphologies of the catalyst were characterized using scanning electron microscopy (HITACHI SU8000). Measurement of BET surface area was performed using N_2 adsorption–desorption isotherms on a Micromeritics (Norcross, GA). The X-ray diffraction (XRD) patterns of $CdFe_2O_4$ powders were recorded on Siemens D5000 Diffractometer (Germany). Vibrating sample magnetometer (VSM, Lakeshore 7407) was used to measure the magnetic prosperities of $CdFe_2O_4$. A Malvern Zetasizer Nano-ZS particle analyzer (Malvern, U.K.) was used to determine the ζ potential of $CdFe_2O_4$. UV-Vis diffuse reflectance spectrum (DRS) was acquired by a UV2550 (Shimadzu Scientific Instruments Inc. Japan) and $BaSO_4$ was used as the reflectance standard. A conventional three electrode cells using a CHI660D electrochemical workstation (Shanghai Chenhua, China) was used to determine the flat-band potential (V_{fb}) of the sample. The working electrode was prepared by dip-coating method as following: 10 mg sample was suspended in 10 mL deionized water, which was then dip-coated onto a 1 cm × 1 cm fluorine–tin oxide (FTO) conducting glass electrode, while a platinum wire as counter electrode, and a standard Ag/AgCl in saturated KCl as reference electrode. The Mott–Schottky measurements were carried out from −1.0V to 1.0V.

2.3. Degradation tests and analytical methods

The experiments were carried out in a temperature-controllable microwave oven (XH100B, Beijing XiangHu Ltd. China) equipped with a reflux condenser. At the beginning, 50 mL of CR (20 mg L^{-1}) aqueous solution and 0.05 g of $CdFe_2O_4$ were added into a 250 mL round bottom flask with 3 necks. Then set up the parameters of the MW oven: power (700 W), temperature (100 °C). CR solution samples during the degradation were taken out at predetermined time intervals by magnetic separation. The degradation of CR under MW irradiation without any catalysts and the CR adsorption on $CdFe_2O_4$ without MW irradiation were also carried out for comparison.

Cary 5000 UV-Vis-NIR (Varian, USA) was utilized to record the spectra of aqueous CR solution after treatment. The reaction intermediates were detected by HPLC (Agilent 1100, USA) equipped with diode array detector and a column oven. A 150 mm × 4.6 mm reverse-phase C-18 column was used for separation. The injection volume was 20 μL, flow rate was 1.0 mL min^{-1}, UV detector wavelength was 497 nm and column oven temperature maintained at 30 °C. The compounds were eluted with methanol–water (38/62 (v/v)).

For further validating degradation of CR in aqueous solution, the ionic chromatogram was used. The other conditions were as follows: AS9-HC column (250 mm × 4 mm i.d.), 9.0 mmol L^{-1} Na_2CO_3 eluent, 1.0 mL min^{-1} flow rate and conductivity detector.

2.4. Analysis of hydroxyl radicals

The formation of hydroxyl radicals on the surface is measured by the fluorescence method, which uses terephthalic acid as a probe molecule.[21,29] Terephthalic acid readily reacted with hydroxyl radicals to produce highly fluorescent product, 2-hydroxyterephthalic acid. The intensity of the fluorescence signal at 425 nm of 2-hydroxyterephthalic acid was in proportion to the amount of hydroxyl radicals produced in water. Fluorescence spectra of the generated 2-hydroxyterephthalic acid were measured on a Cary Eclipse fluorescence spectrophotometer (VARIAN Co, USA).

3. Results and discussion

3.1. Characteristics of $CdFe_2O_4$

Fig. 1a shows the XRD pattern of as-synthesized $CdFe_2O_4$ powders. It is observed that the diffraction peaks could be well indexed to the spinel-type of $CdFe_2O_4$ (JCPDS 22-1063). The diffraction peak appeared below 25° indicated the presence of α-Fe_2O_3. Fig. 1b displays SEM micrograph of the obtained $CdFe_2O_4$, showing the spherical formation of the synthesized nanoparticles with diameter in the narrow size range of 20–30 nm. Some agglomerates of the $CdFe_2O_4$ particles are also observed because of the high surface energy and magnetic interactions between the nanocrystallites. The specific area of the sample was calculated using the Brunauer–Emmett–Teller (BET) method. Fig. 1c displays the N_2 adsorption–desorption isotherm curve of the $CdFe_2O_4$. The BET surface area of $CdFe_2O_4$ was estimated to be 85.80 m^2 g^{-1}. The pore-size distribution of the samples was calculated by Barreet–Juyner–Halenda (BJH) method (see the inset of Fig. 1c). It can be seen that the average pore diameter of $CdFe_2O_4$ is 24 nm. The mesoporous structures would help the adsorption and transition of CR or its intermediates during the degradation process. Fig. 1d presents the hysteresis loops of the $CdFe_2O_4$ (inset: the photo of magnetic separation). The saturation magnetization of $CdFe_2O_4$ is 22.34 emu g^{-1}. Since saturation magnetization of 16.3 emu g^{-1} was enough to separate magnetic particles from solution with a magnet,[30] $CdFe_2O_4$ could be rapidly recovered from water. The UV-Vis diffuse reflectance spectrum of $CdFe_2O_4$ is illustrated in Fig. 1e. The plot obtained by the transformation based on the Kubelka–Munk function *versus* the energy of light is displayed in Fig. 1f. The estimated band gap value (E_g) was 1.97 eV for $CdFe_2O_4$.

3.2. Degradation of CR by $CdFe_2O_4$ with MW irradiation

Fig. 2a shows the change of absorption spectra of CR in the presence of $CdFe_2O_4$. The absorption peak at λ = 497 nm

diminished gradually with increasing irradiation time and completely disappeared after 10 min. No new absorption bands appeared in either the visible or the ultraviolet regions, which indicated the complete decolorization of CR during the reaction.

The removal efficiency of CR over different conditions as a function of time was investigated (Fig. 2b). Self-degradation of CR was almost negligible without catalyst. And the removal efficiency of CR was approximately 26.5% after 10 min in $CdFe_2O_4$ dispersion without MW irradiation. Whereas $CdFe_2O_4$ displayed high catalytic performance, as almost 94.4% of CR was degraded under MW irradiation for only 10 min.

Fig. 2c shows the kinetic studies of the degradation of CR over different conditions. It was observed that the catalytic reaction obeyed the pseudo-first-order model according to the Langmuir–Hinselwood model and may be expressed as:

$$\ln(C_0/C) = kt \quad (1)$$

where C is the concentration of dye at various time (t), C_0 is the initial dye concentration and k is the apparent reaction rate constant of dye removal. The results clearly demonstrated the k value was 26.71×10^{-2} min^{-1} in MW/$CdFe_2O_4$ system. However, the k value was almost negligible with only MW irradiation, proving $CdFe_2O_4$ to be an excellent microwave catalyst.

3.3. Influences of several factors

3.3.1. Effect of initial concentration and catalyst doses. The effects of different initial concentrations of CR on the degradation ratio were examined in the concentration ranges from 20 to 70 mg L^{-1}. Fig. 3a clearly shows that the degradation ratios decrease with increased CR concentration, from 94.4% at initial CR concentration of 20 mg L^{-1} to 46.8% at 70 mg L^{-1} after 10 min MW irradiation. With the initial concentration increase, more organic substances are adsorbed on the surface of the catalyst, but the microwave irradiation time and catalyst are constant.

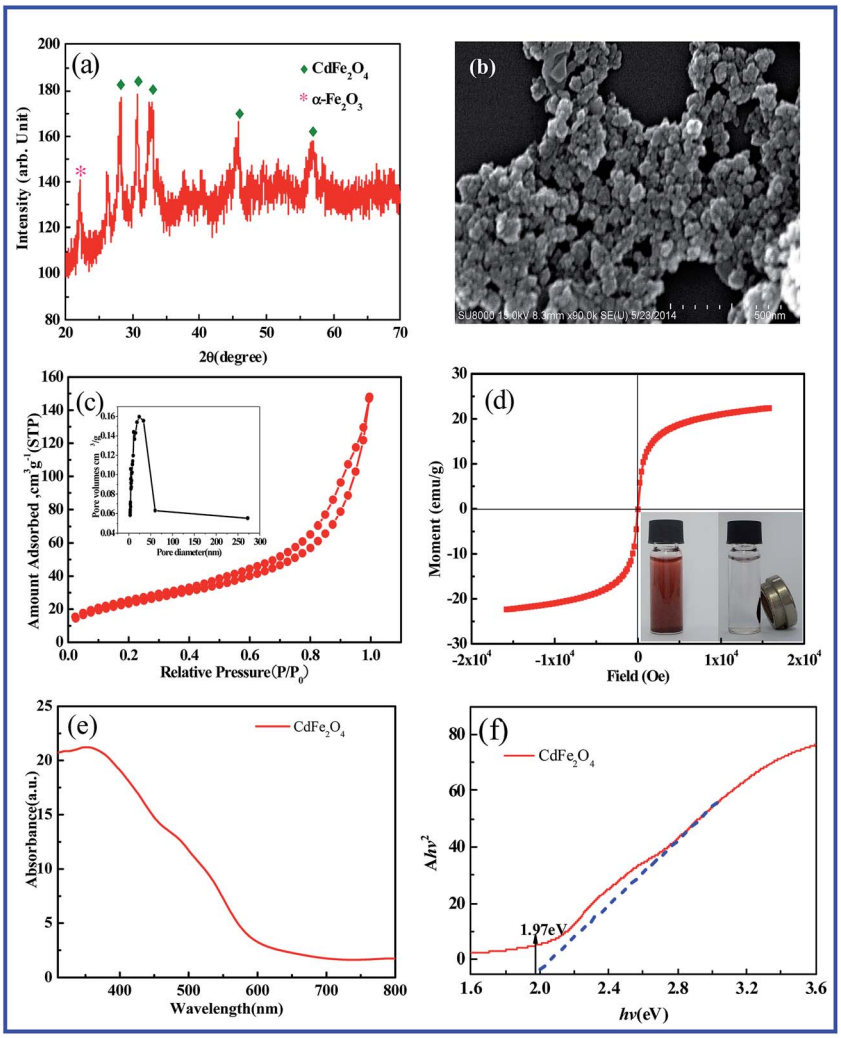

Fig. 1 Characterization of $CdFe_2O_4$. (a) XRD spectrum; (b) SEM image; (c) N_2 adsorption–desorption isotherm. The inset showed the corresponding pore-size distribution; (d) magnetic hysteresis loops (inset: the photo of magnetic separation); (e) UV-Vis diffuse reflectance spectrum (DRS) of $CdFe_2O_4$; (f) plot of transformed Kubelka–Munk function *versus* the energy of light.

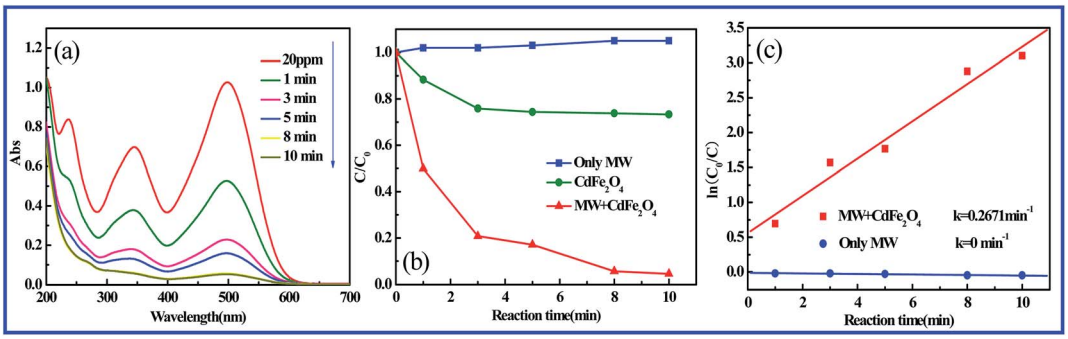

Fig. 2 (a) The variation of UV-Vis absorption spectra at different irradiation time; (b) removal efficiency of CR at different conditions; (c) the kinetic curves.

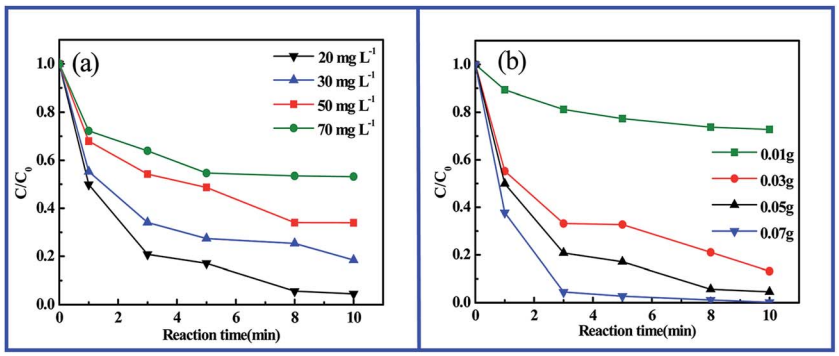

Fig. 3 The effect of the initial concentration (a) and dosage of $CdFe_2O_4$ (b) on the degradation of CR.

Fig. 3b shows the dependence of CR (20 mg L^{-1}) degradation on the dosage of the $CdFe_2O_4$ catalyst. It was found that the degradation ratios increase with increased dosage of $CdFe_2O_4$. And when the dosage exceeded 0.05 g, further increasing the dosage had negligible effect on the degradation ratio of CR after 10 min MW irradiation. Therefore, 0.05 g $CdFe_2O_4$ was used in our experiments.

3.3.2. Effect of microwave power and initial pH. The MW output power was regarded as the most important factor in the experiment, since the temperature that the $CdFe_2O_4$ could reach was directly related to the power level. The investigated power levels were 200, 400, 600 and 700 W, and other parameters remained constant, namely, CR aqueous solution (20 mg L^{-1}) and 0.05 g $CdFe_2O_4$, irradiation time 10 min. The test results shown in Fig. 4a indicated that degradation efficiency of CR gradually increased with the MW power from 200 to 700 W. So the output power of 700 W was chosen in this study.

The influence of initial solution pH on CR degradation was also studied at catalyst dosage 0.05 g, CR concentration 20 mg L^{-1}. Different experiments were performed at pH values of 4.0, 5.0, 7.0, 9.0, and 10.0 as shown in Fig. 4a. It was found that the degradation ratio of CR under MW irradiation changed scarcely and maintained a high level from pH 4.0 to pH 7.0, and then fell slightly after pH 9.0. In general, the natural pH of CR solution was close to 6.5. In this work, the CR solution without adjusting pH was popularly adopted.

The pH of the solution influenced the adsorption behavior of the organic dyes on the catalyst surface. When the pH value is lower than isoelectric point (pH 5.4, Fig. 4b) of $CdFe_2O_4$, its surface is positively charged. Whereas, when the pH value is higher than the isoelectric point, its surface is negatively charged. Therefore, in the acidic and neutral solution the CR anions are close to the surface of $CdFe_2O_4$ particles or adsorbed on it. Hence, the results exhibited a high degradation ratio of CR before pH 7.0. However, at higher pH values the CR anions were generally excluded away from the negatively charged surface of $CdFe_2O_4$. So the degradation ratio began to decrease.

3.3.3. Effect of anions. The existence of inorganic anions such as chloride, sulfate, bicarbonate, nitrate, and acetate is considerably common in wastewaters and also in natural water. In this study, the initial pH 6.5 was employed and the effect of Cl^- on the degradation of CR was studied by adding NaCl into the reaction solution at different concentrations of 0.001, 0.01 and 0.1 mol L^{-1}. The results are shown in Fig. 5a. It can be seen that Cl^- has a detrimental effect at high concentrations of chloride (>0.1 mol L^{-1}). The degradation efficiency of CR without additives is 94.4% after MW irradiation for 10 min, while decreases to 76.6% at $[Cl^-] = 0.1$ mol L^{-1}. The observed inhibition effect can be explained with the scavenging of $^{\cdot}OH$ radicals by ions.[31]

Fig. 5b shows the effects of different anions (*i.e.* SO_4^{2-}, NO_3^-, HCO_3^-, and CH_3COO^-) of their sodium salts at the same concentration of 0.001 mol L^{-1}. Compared to the control test in

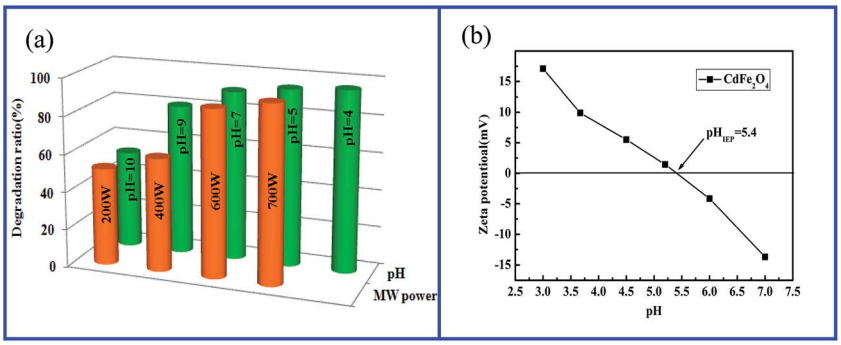

Fig. 4 (a) The effect of microwave power and pH on the degradation of CR; (b) zeta potential of $CdFe_2O_4$.

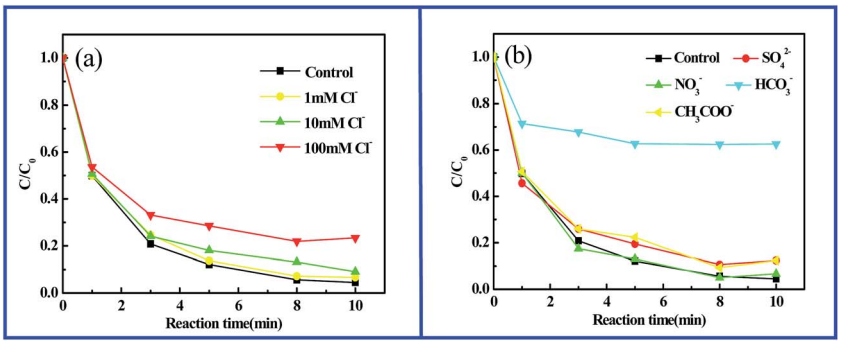

Fig. 5 (a) Influence of Cl^- concentrations on the degradation of CR (initial pH 6.5 and $[C_0] = 20$ mg L^{-1}); (b) degradation of CR in the presence of different anions (initial pH 6.5 and $[C_0] = 20$ mg L^{-1}).

the aqueous CR solutions without anion, NO_3^-, SO_4^{2-}, and CH_3COO^- have no obvious influence on the CR degradation. And the existence of 0.001 mol L^{-1} HCO_3^- leads to the significant retardation of CR degradation, which can be attributed to the combination of radicals scavenging and competitive adsorption. HCO_3^- can be adsorbed by the catalyst. In addition, h^+ and $^{\bullet}OH$ can be trapped by HCO_3^- (eqn (2) and (3)).

$$HCO_3^- + h^+ \rightarrow {}^{\bullet}HCO_3^- \quad (2)$$

$$HCO_3^- + {}^{\bullet}OH \rightarrow {}^{\bullet}HCO_3^- + OH^- \quad (3)$$

3.4. Stability and reusability of $CdFe_2O_4$

The reusability of the catalyst is crucial in the practical application. To evaluate the catalytic stability of $CdFe_2O_4$, the particles were recovered using an external magnet to perform with successive tests of CR degradation. The morphologies of the $CdFe_2O_4$ after reaction were then examined. As shown in Fig. 6a, recycled $CdFe_2O_4$ showed strong activity in CR degradation and its activity remained almost unchanged in four cycles. The degradation ratios in all four runs are more than 90.0%. And the SEM image (Fig. 6b) shows that the sample still maintains the original morphology and particle size. These results strongly

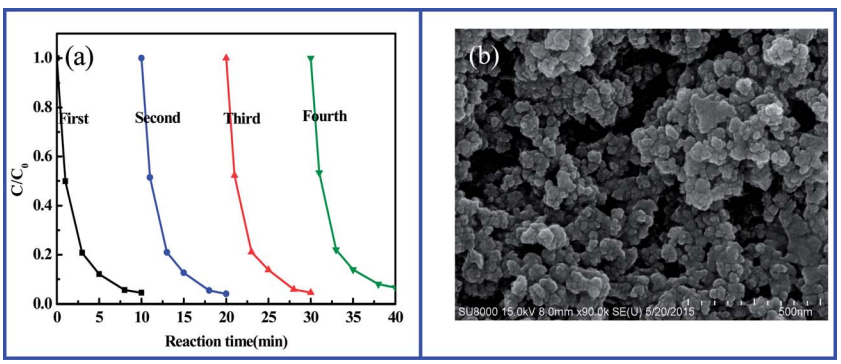

Fig. 6 (a) Cyclic tests of the $CdFe_2O_4$ magnetic catalyst; (b) SEM image of the $CdFe_2O_4$ after the experiment of CR degradation.

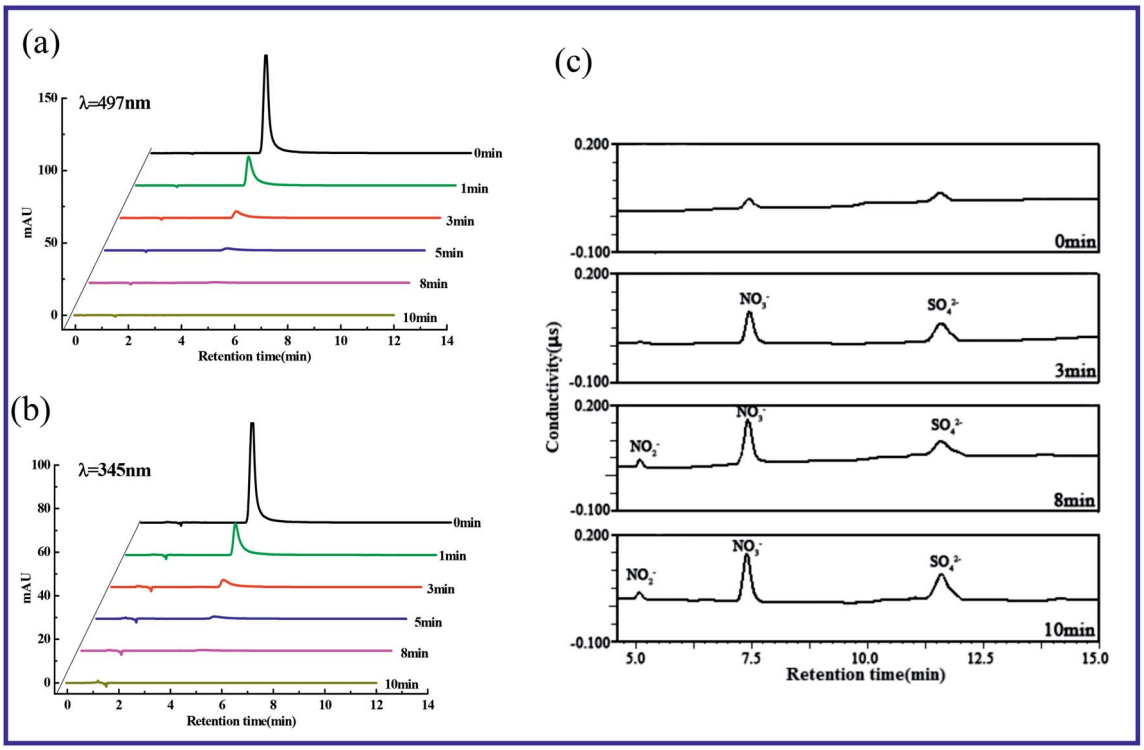

Fig. 7 Variations of HPLC chromatograms of CR over $CdFe_2O_4$ with detection wavelength as 497 nm (a) and 345 nm (b); ion chromatogram of CR solution during degradation (c).

indicate that the $CdFe_2O_4$ nanoparticles are stable and recoverable as catalyst under MW irradiation.

3.5. Identification of the intermediates and final products

In order to explore the intermediates in the degradation process, the chromatography of HPLC analysis was carried out at 497 nm and 345 nm, respectively. As shown in Fig. 7a, the matrix peak of CR appeared at $t_R = 4.28$ min retention time, and it diminished gradually along with the increase of the irradiation time, suggesting CR was degraded obviously and rapidly. Synchronously, the peaks with $t_R = 4.28$ min at 345 nm also significantly decreased (Fig. 7b). It could be seen that there was not any new peak appearing compared to the initial CR solution at both 497 nm and 345 nm, indicating no byproducts was identified.

For further validating degradation of CR in aqueous solution, the ionic chromatogram was determined as shown in Fig. 7c. The ionic chromatographic peaks corresponding to NO_2^-, NO_3^- and SO_4^{2-} anions gradually increased along with microwave irradiation. All of these results indicated that the C–S, C–N and azo bonds in the CR molecule were destroyed gradually. The sulfur and nitrogen atoms were oxidized and transferred into NO_2^-, NO_3^- and SO_4^{2-} anions, respectively. By all means, the CR in aqueous solution could be mineralized to a series of simple and innocuous inorganic ions in the end under microwave irradiation in the presence of $CdFe_2O_4$.

3.6. Role of the reactive species

To detect the main active oxidative species responsible for the degradation in the catalytic process, the influence of some radical scavengers on the degradation of CR over $CdFe_2O_4$ under MW irradiation was investigated. The effects of the scavengers on the degradation efficiency of CR are shown in Fig. 8a. It turned out that the catalytic degradation efficiency of CR decreased notably from 94.4% to 49.5% in the presence of 1 mM sodium oxalate ($Na_2C_2O_4$, h^+ scavenger[32]). Meanwhile, the rate of CR degradation (k) decreased obviously from 26.71×10^{-2} to 6.67×10^{-2} min^{-1}, indicating that the holes are the main active species in the catalytic process. In addition, it has been observed that, upon addition of *tert*-butyl alcohol (TBA) (7.9 wt%), the rate of CR degradation decreases effectively ($k =$

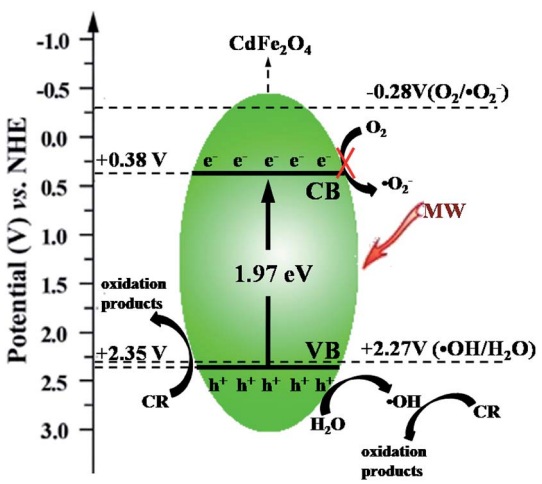

Scheme 1 Possible mechanism for $CdFe_2O_4$ under MW irradiation.

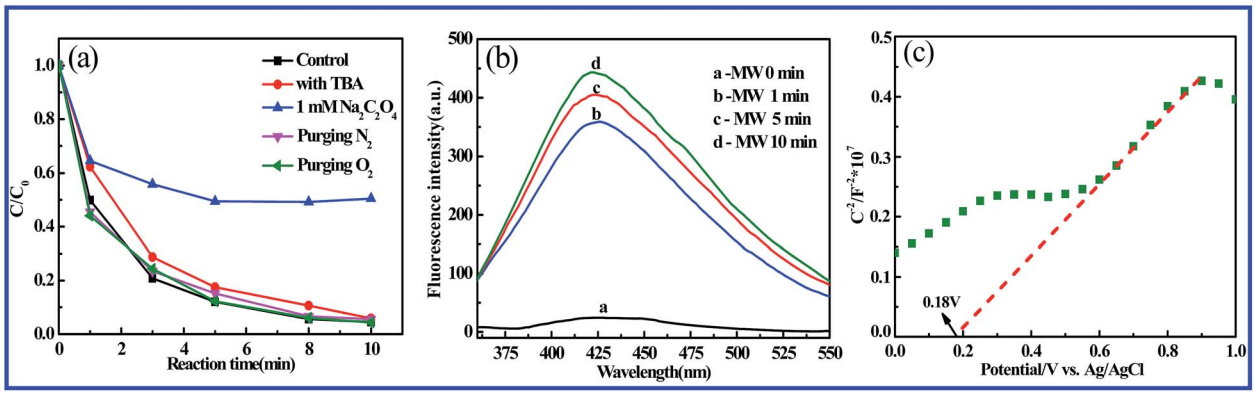

Fig. 8 (a) Effects of a series of scavengers on the degradation efficiency of CR; (b) fluorescence spectral changes with MW irradiation time on $CdFe_2O_4$ in a 3×10^{-4} M basic solution of terephthalic acid. (c) Mott-Schotty plots.

21.54×10^{-2} min^{-1}), which suggested that $^{\bullet}OH$ is also responsible oxidants in degradation of CR. To test the role of $^{\bullet}O_2^-$, N_2 or O_2 was bubbled through the suspension. As shown in Fig. 8a, the negligible effect of N_2 or O_2 bubbling implies that $^{\bullet}O_2^-$ is not the active species in this system.

To further confirm the participation of $^{\bullet}OH$ in degradation of CR, the fluorescence spectrophotometer was used to identify the generated $^{\bullet}OH$ in the microwave-induced catalytic degradation process using terephthalic acid as a probe molecule. Terephthalic acid readily reacts with $^{\bullet}OH$ to produce highly fluorescent 2-hydroxyterephthalic acid (E_x: 315 nm, E_m: 425 nm). Fig. 8b shows the changes of fluorescence spectra from 3×10^{-4} M terephthalic acid solution with irradiation time. A gradual increase in fluorescence intensity at about 425 nm was observed, which further confirmed the production of $^{\bullet}OH$ radicals.

In order to make clear the role of $^{\bullet}O_2^-$ and $^{\bullet}OH$, we also used an electrochemical method to measure the flat-band positions (V_{fb}) of $CdFe_2O_4$. As seen from Fig. 8c, the V_{fb} value is roughly 0.18 V *versus* Ag/AgCl (equivalent to 0.38 V *vs.* NHE). Therefore, it can be determined that the conduction band potential (E_{CB}) of $CdFe_2O_4$ is about 0.38 V. These accumulated electrons on the CB of $CdFe_2O_4$ cannot reduce O_2 to yield $^{\bullet}O_2^-$, because the CB edge potential of $CdFe_2O_4$ (0.38 V *vs.* NHE) was more positive than the standard redox potential $E^{\theta}(O_2/^{\bullet}O_2^-)$ (−0.28 V *vs.* NHE).[33] This explains why N_2 or O_2 bubbling has a negligible effect on the catalytic performance. According to the band gap energy (E_g = 1.97 eV, Fig. 1f) obtained from DRS measurement, the value band potential (E_{VB}) of $CdFe_2O_4$ is deduced to be about 2.35 V *vs.* NHE, which is more positive than $E^{\theta}(^{\bullet}OH/H_2O)$ (2.27V *vs.* NHE).[33] Therefore, the MW-generated holes left behind in the VB of $CdFe_2O_4$ can theoretically oxidize the hydroxyl group or H_2O to produce $^{\bullet}OH$ radicals.

3.7. Possible degradation methism

On the basis of the experimental results mentioned above, a possible catalytic process for the degradation of CR in MW/$CdFe_2O_4$ system could be proposed, as illustrated in Scheme 1. $CdFe_2O_4$ as microwave absorbent can strongly absorb and transfer microwave energy. Under the microwave irradiation, $CdFe_2O_4$ particle surface can produce great amount of "hot spots". Meanwhile, the electrons in $CdFe_2O_4$ could oscillate under the microwave excitation. The "hot-spots" that MW generated could speed up the movement of electrons in $CdFe_2O_4$ to excite electrons and therefore generate electron/hole pairs. The leftover holes directly reacted with CR or interacted with the hydroxyl group or H_2O to produce the $^{\bullet}OH$, which was an extremely strong oxidant for the mineralization of CR. In addition, the holes can also directly oxidize CR to harmless products. Thus, these evidences lead to the conclusion that the holes (h^+) and $^{\bullet}OH$ should be the main factor that responsible for CR oxidation in this system.

4 Conclusion

In this study, $CdFe_2O_4$ has been synthesized by a hydrothermal process and characterized by various techniques such as SEM, XRD, BET VSM and DRS. The as-prepared $CdFe_2O_4$ exhibited excellent catalytic activity in the microwave-induced catalytic degradation process and magnetic property for easy separation using an external magnetic field. The degradation percentage of CR could reach up to 94.4% for 10 min. A possible degradation mechanism is proposed based on the experimental results. This work can provide an effective technology for dye wastewater treatment.

Acknowledgements

This project was supported by the National Nature Science Foundation of China (NSFC51178212), Liaoning Provincial Department of education innovation team projects (LT2012001), the Shenyang Science and Technology Plan (F12-277-1-69), the Foundation of 211 project for Innovative Talent Training, Liaoning University and the Program for Liaoning representative office of China Environmental Protection Foundation (CEPF2013-123-1-5). The authors also thank their colleagues and other students who participated in this work.

References

1 Y. H. Hsien, C. F. Chang, Y. H. Chen and S. Cheng, *Appl. Catal., B*, 2001, **31**, 241–249.
2 U. Zissi and G. Lyberatos, *Water Sci. Technol.*, 1996, **34**, 495–500.
3 Z. Abbasi, M. H. Shariat and S. Javadpour, *Powder Technol.*, 2013, **249**, 181–185.
4 A. Shavandi, A. E. D. A. Bekhit, A. Ali, Z. Sun and J. T. Ratnayake, *Powder Technol.*, 2015, **273**, 33–39.
5 B. Maté, R. D. Suenram and C. Lugez, *J. Chem. Phys.*, 2000, **113**, 192–199.
6 S. Horikoshi, H. Hidaka and N. Serpone, *Environ. Sci. Technol.*, 2002, **36**, 1357–1366.
7 S. Horikoshi, A. Matsubara, S. Takayama, M. Sato, F. Sakai, M. Kajitani, M. Abe and N. Serpone, *Appl. Catal., B*, 2009, **91**, 362–367.
8 T. L. Lai, J. Y. Liu, K. F. Yong, Y. Y. Shu and C. B. Wang, *J. Hazard. Mater.*, 2008, **157**, 496–502.
9 Z. Zhang, Y. Shan, J. Wang, H. Ling, S. Zang, W. Gao, Z. Zhao and H. Zhang, *J. Hazard. Mater.*, 2007, **147**, 325–333.
10 X. Zhang, Y. Wang, G. Li and J. Qu, *J. Hazard. Mater.*, 2006, **134**, 183–189.
11 A. K. L. Sajjad, S. Shamaila, B. Tian, F. Chen and J. Zhang, *J. Hazard. Mater.*, 2010, **177**, 781–791.
12 F. Han, V. S. R. Kambala, M. Srinivasan, D. Rajarathnam and R. Naidu, *Appl. Catal., A*, 2009, **359**, 25–40.
13 X. Quan, X. Liu, L. Bo, S. Chen, Y. Zhao and X. Cui, *Water Res.*, 2004, **38**, 4484–4490.
14 J. E. Atwater and J. R. R. Wheeler, *Appl. Phys. A*, 2004, **79**, 125–129.
15 T. L. Lai, C. C. Lee, K. S. Wu, Y. Y. Shu and C. B. Wang, *Appl. Catal., B*, 2006, **68**, 147–153.
16 L. Zhang, X. Liu, X. Guo, M. Su, T. Xu and X. Song, *Chem. Eng. J.*, 2011, **173**, 737–742.
17 Y. Wu, P. Qiao, J. Qiu, T. Chong and T. S. Low, *Nano Lett.*, 2001, **2**, 161–164.
18 H. Lin, H. Zhu, H. Guo and L. Yu, *Mater. Lett.*, 2007, **61**, 3547–3550.
19 L. Olmedo, P. Hourquebie and F. Jousse, *Adv. Mater.*, 1993, **5**, 373–377.
20 V. M. Petrov and V. V. Gagulin, *Inorg. Mater.*, 2001, **37**, 93–98.
21 X. Li, Y. Hou, Q. Zhao and L. Wang, *J. Colloid Interface Sci.*, 2011, **358**, 102–108.
22 Y. Yao, Y. Cai, F. Lu, F. Wei, X. Wang and S. Wang, *J. Hazard. Mater.*, 2014, **270**, 61–70.
23 J. Deng, Y. Shao, N. Gao, C. Tan, S. Zhou and X. Hu, *J. Hazard. Mater.*, 2013, **262**, 836–844.
24 S. Q. Liu, L. R. Feng, N. Xu, Z. G. Chen and X. M. Wang, *Chem. Eng. J.*, 2012, **203**, 432–439.
25 H. Chen, S. Yang, J. Chang, K. Yu, D. Li, C. Sun and A. Li, *Chemosphere*, 2012, **89**, 185–189.
26 L. Zhang, X. Zhou, X. Guo, X. Song and X. Liu, *J. Mol. Catal. A: Chem.*, 2011, **335**, 31–37.
27 V. Vasanthi, A. Shanmugavani, C. Sanjeeviraja and R. Kalai Selvan, *J. Magn. Magn. Mater.*, 2012, **324**, 2100–2107.
28 F. Miao, Z. Deng, X. Lv, G. Gu, S. Wan, X. Fang, Q. Zhang and S. Yin, *Solid State Commun.*, 2010, **150**, 2036–2039.
29 R. M. Mohamed and E. S. Baeissa, *Appl. Catal., A*, 2013, **464–465**, 218–224.
30 Z. Ma, Y. Guan and H. Liu, *J. Polym. Sci., Part A: Polym. Chem.*, 2005, **43**, 3433–3439.
31 H. C. Liang, X. Z. Li, Y. H. Yang and K.-H. Sze, *Chemosphere*, 2008, **73**, 805–812.
32 B. Jiang, P. Zhang, Y. Zhang, L. Wu, H. Li, D. Zhang and G. Li, *Nanoscale*, 2012, **4**, 455–460.
33 A. Fujishima and X. Zhang, *C. R. Chim.*, 2006, **9**, 750–760.

